amount of a mica-like (same as illite-like) phase (with 1.0-nm spacing) was also observed (*20*) when Fe-rich smectite was chemically reduced by dithionite. However, dithionite is not likely to occur in abundance or to play a substantial role in iron reduction in natural soil environments. In this study, we have shown that bacteria can play an important role in driving the S-I reaction.

A recent study (*21*) demonstrated that *S. oneidensis* MR-1 was able to grow with Fe(III) in the smectite structure as the sole electron acceptor. The S-I reaction was a consequence of a bacterial survival and growth strategy. Iron(III) bound in clay minerals can be an important electron acceptor supporting the growth of bacteria in natural environments. Microbes and clay minerals can coexist in shales, siltstones, and sandstones under diagenetic conditions. Metal-reducing microbes have been discovered in sedimentary rocks from great depths (2700 m below the land surface) (*22*) and in various environments that are hot for microbial survival (up to 90° to 100°C) (*23*). These conditions are similar to those under which clay minerals undergo diagenetic reactions. Natural smectites contain structural Fe(III) to varying degrees (*24*). We suggest that microbial reduction of these quantities of Fe(III) is sufficient to reductively dissolve smectite as a trigger to the S-I reaction.

The microbially promoted S-I reaction should be considered in the study of clay mineral diagenesis. Microbial activity may be responsible for the substantial S-I reaction seen in some modern mudstones, such as those from the Nankai Trough, Japan (*25*). These young sediments have a significant percentage of illite (indicating a large extent of S-I reaction) (*25*) and sulfate-reducing microbes (*26*). It is reported that many sulfate-reducing bacteria can also reduce Fe(III) in mineral structures (*27*). Inorganic reaction is a very slow process under the site conditions.

References and Notes

1. D. R. Pevear, *Proc. Natl. Acad. Sci. U.S.A.* **96**, 3440 (1999).
2. R. L. Freed, D. R. Peacor, *Am. Assoc. Petrol. Geol. Bull.* **73**, 1223 (1989).
3. C. H. Bruce, *Am. Assoc. Petrol. Geol. Bull.* **68**, 673 (1984).
4. K. M. Brown, D. M. Saffer, B. A. Bekins, *Earth Planet. Sci. Lett.* **194**, 97 (2001).
5. R. M. Pollastro, *Clays Clay Miner.* **41**, 119 (1993).
6. C. M. Bethke, S. P. Altaner, *Clays Clay Miner.* **34**, 136 (1986).
7. H. Dong, D. R. Peacor, R. L. Freed, *Am. Mineral.* **82**, 379 (1997).
8. J. L. Keeling, M. D. Raven, W. P Gates, *Clays Clay Miner.* **48**, 537 (2000).
9. C. R. Myers, K. H. Nealson, *Science* **240**, 1319 (1988).
10. J. E. Kostka, J. W. Stucki, K. H. Nealson, J. Wu, *Clays Clay Miner.* **44**, 522 (1996).
11. H. Dong *et al.*, *Environ. Sci. Technol.* **37**, 1268 (2003).
12. E. Gaudett, J. L. Eades, R. E. Grim, *Clays Clay Miner.* **13**, 33 (1966).
13. C. E. Weaver, L. D. Pollard, Eds., *The Chemistry of Clay Minerals* (Elsevier, Amsterdam, 1973).
14. J. F. Buckley, J. C. Bevan, K. M. Brown, L. R. Johnson, V. C. Farmer, *Mineral. Mag.* **42**, 373 (1978).
15. C. M. Warshaw, thesis, The Pennsylvania State University, University Park, PA (1957).
16. D. D. Eberl, R. Nüesch, V. Sucha, S. Tsipursky, *Clays Clay Miner.* **46**, 89 (1998).
17. D. D. Eberl, V. Drits, J. Srodon, R. Nüesch, *U.S.G.S. Open-File Rep.* 96-171, 1996.
18. D. D. Eberl, V. A. Drits, J. Srodon, *Am. J. Sci.* **298**, 499 (1998).
19. E. Eslinger, P. Highsmith, D. Albers, B. DeMayo, *Clays Clay Miner.* **27**, 327 (1979).
20. J. D. Russell, B. A. Goodman, A. R. Fraser, *Clays Clay Miner.* **27**, 63 (1979).
21. J. D. Kostka, D. D. Daulton, H. Skelton, S. Dollhopf, J. W. Stucki, *Appl. Environ. Microbiol.* **68**, 6256 (2002).
22. D. R. Boone *et al.*, *Int. J. Syst. Bacteriol.* **45**, 441 (1995).
23. K. Kashefi, D. E. Holmes, A. L. Reysenbach, D. R. Lovley, *Appl. Environ. Microbiol.* **68**, 1735 (2002).
24. For example, natural smectite ranges from 0.4 mmol of Fe^{3+}/g for Wyoming Na-montmorillonite (Swy-1), to 0.5 mmol of Fe^{3+}/g for Upton montmorillonite, ~1 mmol of Fe^{3+}/g for Gulf Coast smectites, 3.5 mmol of Fe^{3+}/g for the ferruginous smectite (Swa-1), and 4.3 mmol of Fe^{3+}/g for the smectite used in this study.
25. H. Masuda, D. R. Peacor, H. Dong, *Clays Clay Miner.* **49**, 109 (2001).
26. D. W. Reed *et al.*, *Appl. Environ. Microbiol.* **68**, 3759 (2002).
27. D. R. Lovley, in *Environmental Microbe-Metal Interactions*, D. R. Lovley, Ed. (American Society for Microbiology Press, Washington, DC, 2000), pp. 3–30.

28. We thank M. D. Richardson, D. R. Peacor, and J. W. Stucki for extensive comments and discussion. This work was partially supported by the Naval Research Laboratory (contribution no. 7430-03-04). Acknowledgment is made to the donors of the Petroleum Research Fund, administered by the American Chemical Society, for support (or support in part) of this research to H.D.

Supporting Online Material

www.sciencemag.org/cgi/content/full/303/5659/830/DC1
Materials and Methods
References

3 November 2003; accepted 24 December 2003

Genome-Wide RNAi Analysis of Growth and Viability in *Drosophila* Cells

Michael Boutros,[1]*† Amy A. Kiger,[1]* Susan Armknecht,[1,2] Kim Kerr,[1,2] Marc Hild,[3] Britta Koch,[3] Stefan A. Haas,[4] Heidelberg Fly Array Consortium,[3] Renato Paro,[3] Norbert Perrimon[1,2]‡

A crucial aim upon completion of whole genome sequences is the functional analysis of all predicted genes. We have applied a high-throughput RNA-interference (RNAi) screen of 19,470 double-stranded (ds) RNAs in cultured cells to characterize the function of nearly all (91%) predicted *Drosophila* genes in cell growth and viability. We found 438 dsRNAs that identified essential genes, among which 80% lacked mutant alleles. A quantitative assay of cell number was applied to identify genes of known and uncharacterized functions. In particular, we demonstrate a role for the homolog of a mammalian acute myeloid leukemia gene (*AML1*) in cell survival. Such a systematic screen for cell phenotypes, such as cell viability, can thus be effective in characterizing functionally related genes on a genome-wide scale.

The availability of entire genome sequences stimulates the advancement of functional genomic approaches, both to accelerate the comprehensive identification of components in biological programs and to understand their functional conservation across species (*1*, *2*). In yeast and in worms, genome-wide phenotypic studies identified genes that were essential for cell fitness and development (*3*, *4*). *Drosophila* is one of the best-studied genetic organisms and is instrumental to the identification of conserved pathways with important roles from flies to humans. Treatment of cultured *Drosophila* cells with dsRNA leads to the depletion of the corresponding transcript and the generation of specific and penetrant phenotypes (*5*), providing an efficient approach for systematic loss-of-function phenotypic analyses (*6*–*9*).

Cell growth, proliferation, and survival are fundamental processes that maintain cell populations and impinge on lineage expansion and pattern formation (*10*). To identify gene functions by cell-based RNAi screens, we generated a dsRNA library targeting near-

[1]Department of Genetics, [2]Howard Hughes Medical Institute (HHMI), Harvard Medical School, Boston, MA 02115, USA. [3]Zentrum für Molekulare Biologie der Universität Heidelberg, D-69120 Heidelberg, Germany. The Heidelberg Fly Array Consortium consists of Marc Hild, Boris Beckmann, Stefan Haas, Britta Koch, Martin Vingron, Frank Sauer, Jörg Hoheisel, and Renato Paro. [4]Max-Planck Institute for Molecular Genetics, D-14195 Berlin, Germany.

*These authors contributed equally to this work.
†Present address: German Cancer Research Center, D-69120 Heidelberg, Germany.
‡To whom correspondence should be addressed. E-mail: perrimon@rascal.med.harvard.edu

ly all genes in the *Drosophila* genome (fig. S1). In total, 21,306 primer pairs were designed to amplify gene-specific fragments (*11*) then used for synthesis of dsRNAs (*12*). We established a quantitative assay of cell number that correlated the reduction of signal to dying cells, as demonstrated by RNAi of the *D-IAP1* (*13*) inhibitor of apoptosis (a positive control in screen and data processing; Fig. 1, A and B).

Genome-wide RNAi screens in two embryonic hemocyte (blood cell) lines (*14*, *15*) were each performed in duplicate (Fig. 1C and fig. S2). In total, we analyzed 77,880 RNAi experiments (*12*). A comparison between duplicate screens revealed qualitatively and highly quantitatively reproducible results (Fig. 1D) with a correlation coefficient of 0.86 (Kc_{167} cells, fig. S2). The results included reproducibly subtle to severe phenotypes as quantified by a significance factor, or *z* score (this score signifies the severity or rank of specific RNAi phenotypes) (*12*) (Fig. 1, C and D). For example, *D-IAP1* resulted in a severe phenotype with *z* scores of 6.1 and 7.0 in $S2R^+$ and Kc_{167} cells, respectively. To determine the efficiency of the screen, we assessed the phenotypes for a highly represented functional group of genes. Nearly all of the tested genes encoding ribosomal components exhibited similar quantitative phenotypes (72 genes with a mean *z* score of 2.9 ± 0.8; fig. S3), of which 68 had at least one *z* score greater than 2.2, and 54 greater than 3.0. The phenotypic scores for the total set of ribosomal components were statistically distinguishable from the cell death phenotype of *D-IAP1* ($P < 0.0001$, Fig. 2), showing that differences in *z* scores between selected gene sets can be detected by this method. Quantitative reproducibility of the method was also demonstrated through an analysis of the phenotypes from independent dsRNAs targeting the same gene within one screen. For example, each dsRNA directed against neighboring predicted genes *cpo*, *CG12349*, and *CG18435* exhibited similar phenotypes (*z* scores of 3.6, 3.2, and 3.7, respectively). Consistent with this, current annotation now depicts these three gene models as a single gene (*16*).

To further analyze essential gene functions, we selected 438 cases in which dsRNAs resulted in greatly reduced cell number as represented by a *z* score of 3 or more (Fig. 3A and tables S1 and S2). This threshold included RNAi phenotypes ranging in severity from *z* scores of 3 to 7.7, likely representing defects in cell growth to defects in cell survival. Only 20% (87 out of 438) of the identified genes had associated mutant alleles in *Drosophila*, which included genes with demonstrated roles in cell growth, cell cycle, and anti-apoptotic cell survival (*12*) (table S3), whereas the vast majority lacked mutant alleles for functional analyses.

Of the 438 cases, 47% (206 out of 438) had an associated Gene Ontology annotation (*17*), and 59% (260 out of 438) encoded an identifiable InterPro protein domain (*18*). When the most abundant domain predictions were used to categorize genes into distinct functional classes (Fig. 3B; individual predictions and assignments in tables S1 and S4) (*12*), the relative distribution of predicted gene functions differed with the quantitative severity of the RNAi phenotypes (Fig. 3, B and C).

The phenotypic screen also identified genes encoding sets of proteins in known biochemical complexes, as revealed by sequence-based classification (Fig. 3B). Examples of this were within two of the most abundant categories pertaining to protein translation (56 genes, "Ribosome") and ubiquitylation and protein degradation (34 genes, "Proteasome"). Genes with predicted roles in the cell cycle showed quantitative phenotypes similar to those involved in protein translation, but in only one of the two cell types screened ("Cell Cycle," Fig. 3D; supporting online material text). One of the most populated categories consisted of genes for 62 proteins with predicted DNA binding domains ("DNA binding," Fig. 3B, table S1), including chromatin-related factors (e.g., core Histone and high-mobility group (HMG)–box domains: *bss* and *CG17836*; Fig. 3D) and representative members of transcription factor families (e.g., homeobox, ets, and AML domains: *abd-A*, *aop*, and *CG15455*; Fig. 3D). Only genes for specific transcription factors from within different families were identified. For example, although four different AML-

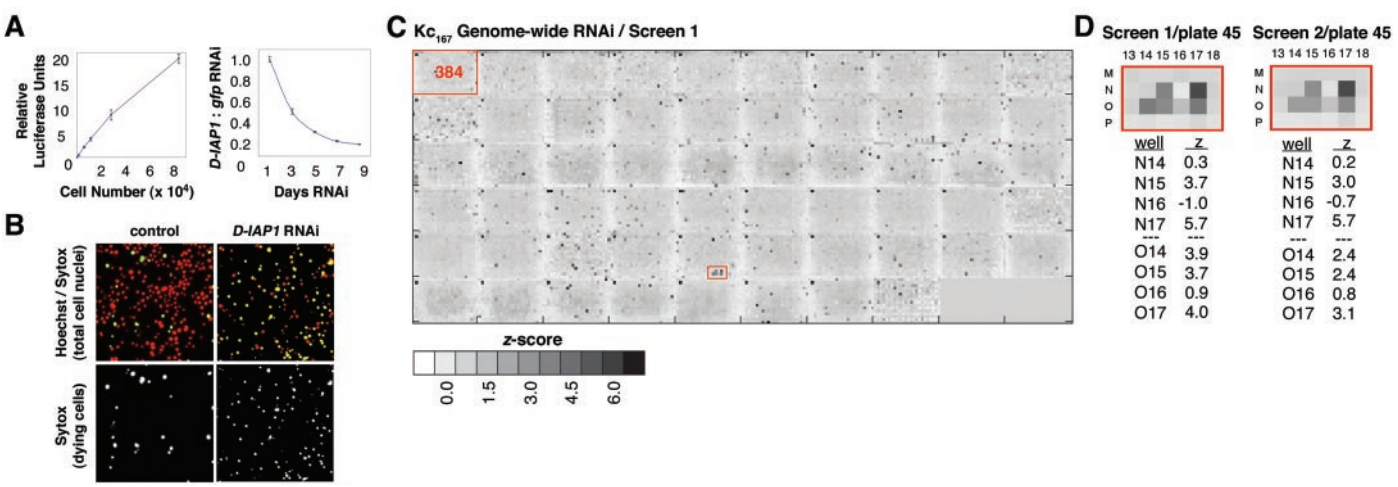

Fig. 1. Genome-wide RNAi screens result in highly reproducible growth and viability defects. Results for Kc_{167} cells are shown; similar results were observed for $S2R^+$ cells (*22*) (table S1). (**A**) Left panel: Luciferase activity (relative light units) indicative of ATP levels is correlated with number of *Drosophila* cells in a high-throughput assay format (fig. S1). Right panel: Treatment with dsRNA targeting *D-IAP1* induced time-dependent decrease in cell viability is shown as the relative readout as compared with cells treated with control *green fluorescent protein* (*gfp*) dsRNA (normalized to 1). (**B**) Fluorescence microscopy of cells after 3 days RNAi. More dying cells were detected after treatment with *D-IAP1* than with control dsRNAs by the ratio of SYTOX green–labeled nuclei (green and lower panel) versus Hoechst 33342–labeled nuclei (red). (**C**) Results from one genome-wide RNAi screen, after 5 days dsRNA treatment. Each RNAi experiment is represented by a shaded box (a single well), arranged by 384-well plates as outlined in upper left. Results in each plate were mean-centered before overall analysis. Gray values indicate *z* score, with darker shades representing below-average results. Each 384-well plate had four control wells containing either *D-IAP1* or the negative controls *gfp*, *Rho1*, or no dsRNAs. The *D-IAP1* control phenotypes are evident as the dark boxes in the upper left corner of each plate, indicative of dying cells and a lower signal. (**D**) Example of highly reproducible phenotypes with similar *z* scores from two independent RNAi screens [enlarged from (C) and from duplicate screen in fig. S2].

like genes are encoded within the fly genome, only one, *CG15455*, was functionally identified in the screen (fig. S4). Serpent, a GATA-1 homolog with roles in fly and mammalian blood cell development and survival (*19*), was identified as the only one of five predicted GATA-type Zinc-finger transcription factors (*srp*, Fig. 3D). Proteins with a predicted DNA binding domain comprised the largest assigned category of genes identified, both in total (14%, Fig. 3B) and in the class with the most severe phenotypes (19%, *z* score > 5, Fig. 3C), an enrichment from the proportion found in the genome (5%).

Overall, the largest category of genes (41%) had no recognizable predicted protein domain (178 genes, "No Prediction," Fig. 3B), suggesting that the screen identified many uncharacterized genes with essential cellular roles (table S1). For example, severe cell viability phenotypes (*z* scores 6.8 and 7.3) were observed with HFA13298 dsRNA targeted against a newly predicted gene, *HDC14318*, with six overlapping expressed-sequence tags mapped to the same region (RH13972, RH23223, RH26651, RH22174, RH26647, and RH62785). The proportion of 438 genes with phenotypes but without a predicted protein domain increased with phenotypic severity (63% "No Prediction," *z* score > 5; Fig. 3C).

We also identified uncharacterized genes with phenotypes quantitatively similar to that of *D-IAP1* (*z* score > 5), raising the possibility that these loss-of-function phenotypes resulted from cell death, perhaps due to the activation of apoptosis. We further evaluated two such genes, *CG11700*, a ubiquitin-like gene, and *CG15455*, a gene encoding an AML1-like transcription factor (*z* scores 7.2 and 7.4 in Kc_{167} cells, respectively, Fig. 3D). The phenotypic severity could not be attributed to an accumulated arrest in transition at one stage in the cell cycle (*12*) (Fig. 4A and fig. S5). As indicated by terminal transferase-labeled DNA breaks, over 95% of cells treated with dsRNA to *CG11700* or *D-IAP1*, and 20% of cells treated with dsRNA to *CG15455*, were apoptotic (*12*) (Fig. 4B). The addition of a pan-caspase inhibitor, Z-Val-Ala-DL-Asp(O-Methyl)-fluoro-

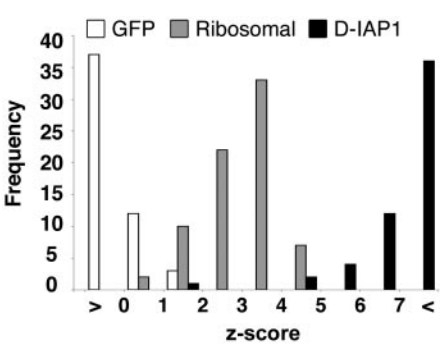

Fig. 2. Similar quantitative RNAi phenotypes of genes encoding ribosomal proteins. Averaged RNAi phenotypes of 72 genes encoding all annotated ribosomal proteins tested (gray bars) are distinguishable from negative controls (white bars, *gfp* dsRNA) and more severe phenotypes (black bars, *D-IAP1* dsRNA). The *gfp* and *D-IAP1* results represent negative and positive control experiments (scored one per plate) over a genome-wide screen. Intergroup comparisons are highly significant in a Student's *t* test ($P < 0.0001$) (fig. S3).

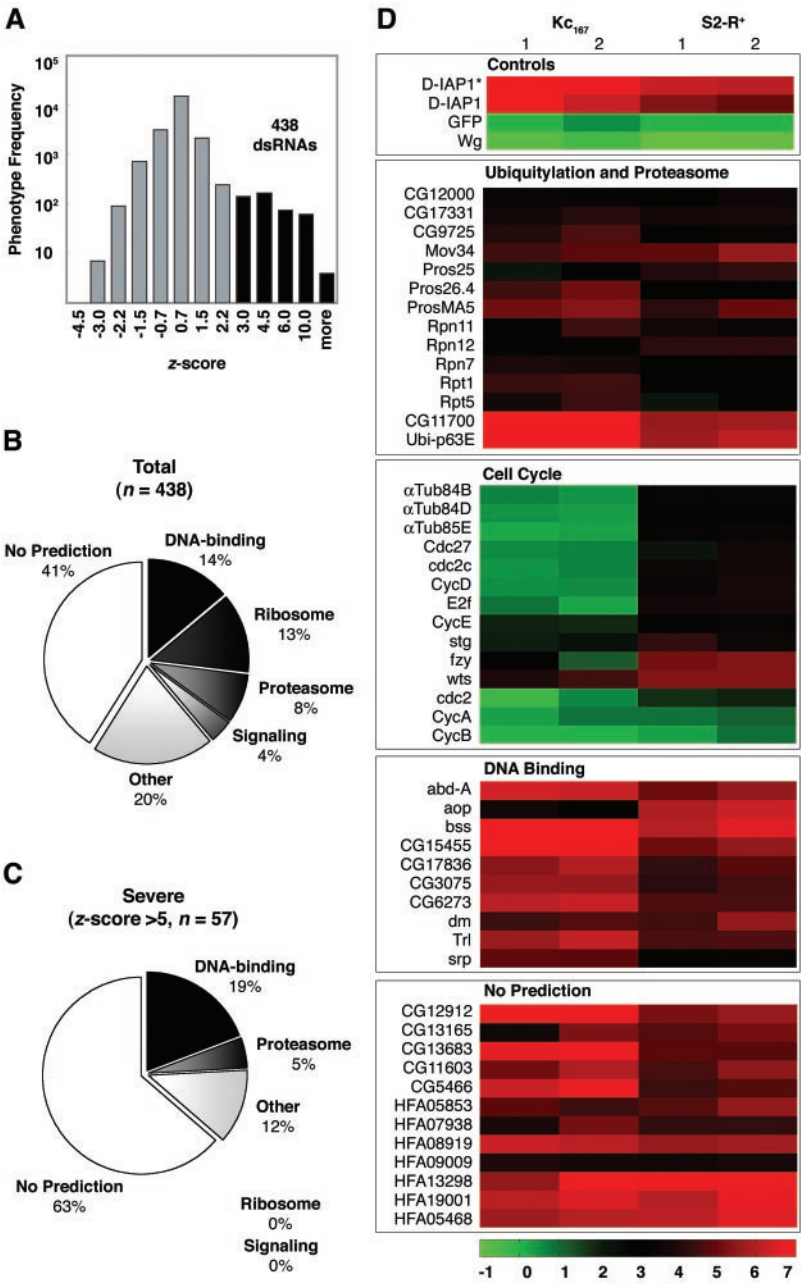

Fig. 3. Quantitative grouping of RNAi phenotypes. (**A**) Distribution of the frequency of RNAi phenotypes recovered for each specified range of *z* scores. We used a *z* score of three or more standard deviations from the mean as a threshold to select 438 results for further analysis (tables S1 and S10). (**B** and **C**) Frequency of encoded functional groups as predicted by InterPro protein domains and manually assigned to representative categories (tables S1 and S4) for all selected phenotypes [(B), *z* score > 3] and the most severe phenotypes [(C), *z* score > 5], revealing significant changes in the abundance of predicted ribosome proteins ($P < 0.001$) and proteins with no predicted domains ($P < 0.00001$). *z* scores were averaged across experiments. (**D**) Classification of quantitative RNAi phenotypes of selected genes (rows) identifies groups of related and new gene functions, as determined from duplicate screens per cell type (columns) and visualized by *z* score (scale, bottom). Both *D-IAP1** (added control) and *D-IAP1* (within RNAi library) yield equivalent phenotypes.

methylketone (z-VAD-fmk), reverted the cell death in response to the RNAi of *CG11700* and *D-IAP1*, and to a lesser extent of *CG15455* and other transcription factors (Fig. 4C). D-IAP1 directly inhibits the proapoptotic caspase, Nc (Nedd2-like) (*20*). The *CG11700* and *D-IAP1* dsRNA-induced cell death phenotypes were both rescued by combined RNAi removing the single *Nc* caspase function (Fig. 4C). In contrast, neither the loss of function of *Nc* (Fig. 4) nor the loss of function of the transcriptionally activated proapoptotic gene *reaper* (*19*, *21*, *22*) (fig. S6) was sufficient to suppress cell death upon co-RNAi with *CG15455* or other tested transcription factors. Together, these results suggest that the ubiquitin-like *CG11700* may act in the same pathway as *D-IAP1* to directly prevent Nc caspase-activated apoptotic cell death. In contrast, a set of essential transcription factors may regulate complex responses for cell fate, proliferation, and/or cell survival that directly or indirectly initiate a partially caspase-dependent apoptotic program.

In comparisons made between complete proteomes (*12*), the percentage of predicted orthologs found for the genes with RNAi viability phenotypes was higher than the percentage of orthologs found in searches of the entire *Drosophila* proteome with those from yeast, worm, mosquito, mouse, and human (fig. S6 and table S5). Notably, 50 genes had homology to human disease genes (table S6), including 10 genes implicated in blood-cell leukemia (e.g., AML1) and genes described with anti-apoptotic functions (FOXOA1 and MLK). Thus, functional analysis in *Drosophila* cells uncovered common key regulators for animal cell survival and proliferative decisions. Interestingly, in contrast to the total results, the most severe RNAi phenotypes (*z* score > 5, fig. S8) identified significantly fewer yeast homologs (from 39 to 19.3%, respectively), a similar percentage of animal-specific homologs (27.6 and 29.8%), and an increased number of genes without high-scoring matches (from 33.3 to 50.9%) (*12*). This suggests that metazoans may have evolved specific mechanisms, such as the preservation of cell identity by a specific code of transcription factors, to maintain cell viability.

Functional analysis by RNAi reveals previously unknown and evolutionarily conserved gene functions, with the powerful ability to comprehensively and quantitatively determine the contribution of potentially every gene to a particular process. Quantitative cell-based analysis offers advantages by permitting the detection of gene functions associated with subtle or redundant phenotypes in organisms. This approach also holds the potential for statistical clustering across many different cellular phenotypes to elucidate complex gene functions as more data accumulate (*23*). The described genome-wide RNAi library is adaptable for screening for many different cellular pathways and processes, ultimately leading to a functional understanding of cellular systems that control development and disease.

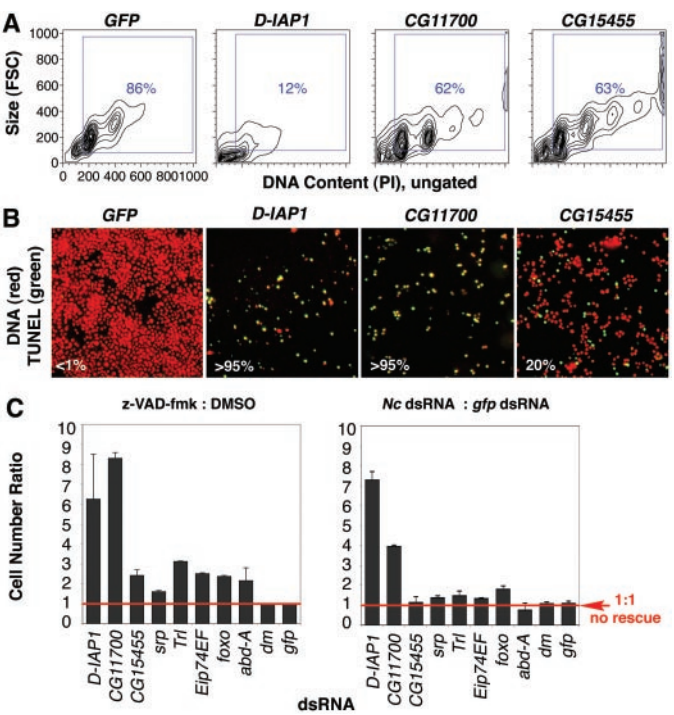

Fig. 4. Different anti-apoptotic gene functions identified by severe RNAi viability phenotypes. Experiments shown as assayed in Kc_{167} cells following RNAi against a negative control (*gfp*) and *D-IAP1*, *CG11700* (ubiquitin-like), and *CG15455* (AML-1-like, fig. S4) genes, each identified in the screen by severe phenotypes (*z* scores 7.0, 7.2, and 7.4, respectively). (**A**) Flow cytometry analysis of propidium iodide (PI) stained DNA after 3 days RNAi, as indicated (*12*). Analyses of total events reveal decreased cell size and DNA content, indicative of dying cells. Cell cycle distribution analysis performed on viable cells with ≥2*N* DNA content [percentage of total events shown, fig. S5 (*12*)]. FSC, forward scatter channel. (**B**) Two classes of severe RNAi phenotypes were distinguished by the proportion of apoptotic cells (>95 and 20%), as indicated by fluorescein-labeled dsDNA breaks [terminal deoxynucleotidyl transferase–mediated deoxyuridine triphosphate nick end labeling (TUNEL), green and lower panel] versus total cell nuclei (Hoechst 33342 DNA stain, red) 7 days after treatment with dsRNAs. (**C**) Left panel: Rescue of RNAi growth and viability phenotypes by a pan-caspase inhibitor (z-VAD-fmk). Shown are the ratios between combined treatments with dsRNA and either z-VAD-fmk in dimethyl sulfoxide (DMSO), or in DMSO alone (red line, normalized to 1), from results of averaged triplicate experiments. Right panel: Data are displayed as in the left panel, but they are from combined treatments with test dsRNA and either dsRNA against *Nc* caspase or *gfp* control.

References and Notes

1. S. A. Chervitz *et al.*, *Science* **282**, 2022 (1998).
2. T. R. Golub *et al.*, *Science* **286**, 531 (1999).
3. G. Giaever *et al.*, *Nature* **418**, 387 (2002).
4. R. S. Kamath *et al.*, *Nature* **421**, 231 (2003).
5. J. C. Clemens *et al.*, *Proc. Natl. Acad. Sci. U.S.A.* **97**, 6499 (2000).
6. M. Ramet, P. Manfruelli, A. Pearson, B. Mathey-Prevot, R. A. Ezekowitz, *Nature* **416**, 644 (2002).
7. M. P. Somma, B. Fasulo, G. Cenci, E. Cundari, M. Gatti, *Mol. Biol. Cell* **13**, 2448 (2002).
8. L. Lum *et al.*, *Science* **299**, 2039 (2003).
9. A. Kiger *et al.*, *J. Biol.* **2**, 27 (2003).
10. M. Guo, B. A. Hay, *Curr. Opin. Cell Biol.* **11**, 745 (1999).
11. M. Hild *et al.*, *Genome Biol.* **5**, R3 (2003).
12. Materials and methods are available as supporting material on *Science* Online. Complete protocols and data sets are also provided on http://drsc.med.harvard.edu/viability.
13. B. A. Hay, D. A. Wassarman, G. M. Rubin, *Cell* **83**, 1253 (1995).
14. G. Echalier, A. Ohanessian, *In Vitro* **6**, 162 (1970).
15. S. Yanagawa, J. S. Lee, A. Ishimoto, *J. Biol. Chem.* **273**, 32353 (1998).
16. S. Misra *et al.*, *Genome Biol.* **3**, RESEARCH0083 (2002).
17. FlyBase Consortium, *Nucleic Acids Res.* **31**, 172 (2003). FlyBase, a database of the *Drosophila* genome, is available at www.flybase.org.
18. N. J. Mulder *et al.*, *Nucleic Acids Res.* **31**, 315 (2003). InterPro, a database of protein families, domains, and functional sites, is available at www.ebi.ac.uk/interpro.
19. L. H. Frank, C. Rushlow, *Development* **122**, 1343 (1996).
20. I. Muro, B. A. Hay, R. J. Clem, *J. Biol. Chem.* **277**, 49644 (2002).
21. K. White, E. Tahaoglu, H. Steller, *Science* **271**, 805 (1996).
22. M. Boutros *et al.*, data not shown.
23. F. Piano *et al.*, *Curr. Biol.* **12**, 1959 (2002).

24. We thank T. Mitchison and the Institute of Chemistry and Cell Biology for advice on cell-based screens and usage of equipment; L. Hrdlicka and S. Hagar for excellent technical support; R. Steen for use of equipment; L. Kockel, B. Gelbart, and D. Emmert for constructive discussions; and G. Rubin, T. Ingolia, P. Leder, T. Mitchison, A. McMahon, L. Perkins, R. Tanis, M. Vincent, and B. Ward for support at various stages of this project. Supported by HHMI, as well as a gift from M. Crowinshield and additional support from Harvard Medical School. Work in R.P. laboratory was supported by the German Human Genome Project (DHGP). M.B. was supported by an Emmy-Noether grant from the Deutsche Forschungsgemeinschaft. A.K. was supported by The Jane Coffin Childs Memorial Fund for Medical Research.

Supporting Online Material

www.sciencemag.org/cgi/content/full/303/5659/832/DC1
Materials and Methods
SOM Text
Figs. S1 to S8
Tables S1 to S8

8 September 2003; accepted 23 December 2003

Genome-Wide RNAi Analysis of Growth and Viability in *Drosophila* Cells

Michael Boutros, Amy A. Kiger, Susan Armknecht, Kim Kerr, Marc Hild, Britta Koch, Stefan A. Haas, Heidelberg Fly Array Consortium, Renato Paro and Norbert Perrimon (February 5, 2004)

Science **303** (5659), 832-835. [doi: 10.1126/science.1091266]

Editor's Summary

Science (print ISSN 0036-8075; online ISSN 1095-9203) is published weekly, except the last week in December, by the American Association for the Advancement of Science, 1200 New York Avenue NW, Washington, DC 20005.